ECS Transactions, 35 (1) 2129-2136 (2011)
10.1149/1.3570204 ©The Electrochemical Society

Investigation of Cathode Kinetics in SOFC: Model Thin Film $SrTi_{1-x}Fe_xO_{3-\delta}$ Mixed Conducting Oxides

W. Jung[a] and H. L. Tuller

Department of Materials Science and Engineering, Massachusetts Institute of Technology
Cambridge, Massachusetts 02139, USA
[a] Present address: Applied Physics and Materials Science, Caltech
Pasadena, California 91125, USA

To understand the kinetics controlling the SOFC cathode processes, a model mixed conducting perovskite materials system, $SrTi_{1-x}Fe_xO_{3-\delta}$, was selected, offering the ability to systematically control both the levels of electronic and ionic electrical conductivity as well as the energy band structure. This, in combination with considerably simplified electrode geometry, served to demonstrate that the rate of oxygen exchange at the surface of $SrTi_{1-x}Fe_xO_{3-\delta}$ is only weakly correlated with either high electronic or ionic conductivity, in apparent contradiction with common expectations. On the other hand, evidence was found suggesting the importance of minority electronic species in determining the rate of oxygen exchange. Furthermore, the enrichment of Sr to the surface of the electrodes was found to reduce the oxygen exchange rate constant; this effect becoming more evident with increasing values of x. The observed trends are discussed in relation to the cathodic behavior of MIEC electrodes.

Introduction

Identifying the important factors governing oxygen reduction kinetics at solid oxide fuel cell cathodes is critical for enhanced performance, particularly at reduced temperatures. In this work, the $SrTi_{1-x}Fe_xO_{3-\delta}$ system (STF) was selected, offering the ability to systematically control both the levels of ionic and electronic conductivity as well as the energy band structure. This, in combination with considerably simplified electrode geometry, is demonstrated to provide improved insight into the SOFC cathode processes. For this purpose, dense thin film STF cathodes, with compositions x=0.05 to 1, were prepared by pulsed laser deposition, and their cathode reaction kinetics examined as a function of electrode geometry, temperature, pO_2 by means of electrochemical impedance spectroscopy (EIS). Previously, the authors demonstrated that a number of thin film STF compositions, when operated as a cathode, exhibit typical mixed ionic-electronic behavior with the electrode reaction occurring over the full electrode surface area rather than being limited to the triple phase boundary. By changing electrode geometries and inserting a $Ce_{0.9}Gd_{0.1}O_{2-\delta}$ (CGO) interlayer, the surface oxygen exchange reaction was confirmed to be the rate limiting process, as is generally the case for mixed ionic-electronic conductors (MIEC) [1,2].

In the present contribution, the surface oxygen exchange kinetics, obtained from impedance spectroscopy data, were correlated with ionic and electronic transport

properties, electronic band structure, and surface chemical properties of STF electrodes over a wide range of x in STF and as functions of T & pO_2. Based on the observed findings, some suggestions regarding criteria required for optimum MIEC SOFC cathode performance are proposed.

Experimental

Sample Preparation and Characterization

STF thin films were prepared by means of pulsed laser deposition (PLD) from oxide targets of the respective materials and deposited onto (100) oriented single crystal yttria doped zirconia (YSZ) substrates for EIS measurement. Deposition conditions have been reported previously [1,2].

The resulting polycrystalline films exhibited the perovskite structure with highly (110) orientated texture as confirmed by X-ray diffraction (Rigaku RU300). There is no evidence of amorphous films, or diffraction peaks other than the ones in the cubic perovskite phase. The grain sizes were determined to fall within the range of 100-200 nm by atomic force microscopy (Digital Instruments Nanoscope IIIa) and the RMS surface roughness was calculated to be less than 1 nm (e.g., 0.75 ± 0.12 nm) for a 500 nm thick layer, indicative of a highly smooth surface. Film thicknesses ranging between 70 and 440 nm were determined by surface profilometry (Tencor P-10).

The chemical composition of the sample surfaces were measured in a Kratos Analytical (Manchester, UK) model Axis Ultra x-ray photoelectron spectrometer. A monochromated aluminum x-ray source of 1486.6 eV was used at a power of 150 W. Pass energy of 160 eV and 20 eV were used for survey and high resolution scans, respectively. Binding energy values were calibrated by setting the peak energy of the 1s electron in carbon, found as a surface contaminant in open air, to 285.0 eV. For depth-dependent composition determination, an Ar ion beam of 4 kV was used with 2 x 2 mm^2 rastering area.

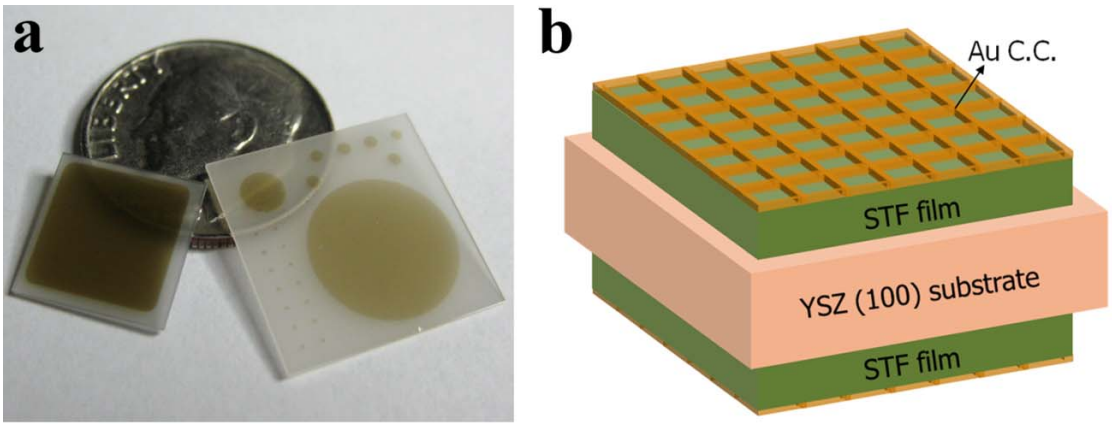

Figure 1. A photograph (a) and a schematic illustration (b) of the symmetrical structures of STF thin films together with Au current collectors (C.C.) deposited on top of single crystal YSZ substrates.

Electrical and Electrochemical Impedance Spectroscopy (EIS) Measurements

A symmetrical structure, with identically sized STF electrodes on both sides of the YSZ electrolyte, was used for EIS measurements (see Figure 1a-b). Au mesh and Au paste were placed on each STF electrode surface, serving as current collectors. Both a custom-designed enclosed probe station, manufactured by McAllister Technical Services (Coeur d'Alene, ID) and a tube furnace were used for the EIS measurements at temperatures between 570°C and 650°C and between 2 x 10^{-5} atm to 1 atm. EIS measurements, covering the frequency range from 7 mHz to 1 MHz, with amplitude of 20 mV, were performed with a Solarton 1260 or 1250 impedance analyzer operated in combination with a Solartron 1286 potentiostat/galvanostat. The conductivity measurements were performed under the same conditions with four sputtered Pt electrode with the aid of a HP 3478A multimeter.

Results and Discussion

Values for Area Specific Resistance and Surface Exchange Coefficient (*k*)

The area specific resistance R_{STF}, extracted from the EIS measurements in air, is plotted as a function of reciprocal temperature in Figure 2 as a function of the STF Fe fraction. For a detailed discussion of how the impedance spectra of these thin film structures are analyzed, the reader is referred to previous publications by the authors [1, 2]. Since the STF electrode resistance is governed by the surface oxygen exchange reaction, R_{STF} is an indicator of the oxygen surface exchange rate. The corresponding kinetic parameter *k* (surface oxygen exchange coefficient) may be extracted from the measured electrode resistance, according to equation 1 as [3];

$$k = \frac{k_B T}{4e^2 R_S c_O} \quad (1)$$

(k_B: Boltzmann constant, *e*: electron charge, *T*: temperature, R_s: area specific resistance and c_o: total concentration of lattice oxygen with the value 4.92 x 10^{22} cm^{-3} used in this calculation [4]).

While there is reduction in R_{STF} (or increase in *k*) with increasing Fe composition, the rate of change decreases so that R_{STF} reaches near saturation above x=0.35 (STF35). For comparison, the *R* values for dense thin films of the more typical MIEC cathodes prepared by PLD are also inserted in Figure 2. The area specific resistance values of the thin film STF electrodes are found to be comparable in magnitude to those of thin film $La_{0.6}Sr_{0.4}Co_{0.2}Fe_{0.8}O_3$ (LSCF), the most commonly used MIEC cathode material at intermediate temperatures, pointing to the suitability of STF as a realistic model mixed conducting cathode material [5-8]. Surprisingly, this is true even though the electronic conductivity (σ_{el}) of the STF cathodes is as much as 5 orders of magnitude lower than that of LSCF (σ_{el} = 330 S/cm at 650°C, k^* = 6 ×10^{-7} cm/s at 663°C) [9,10].

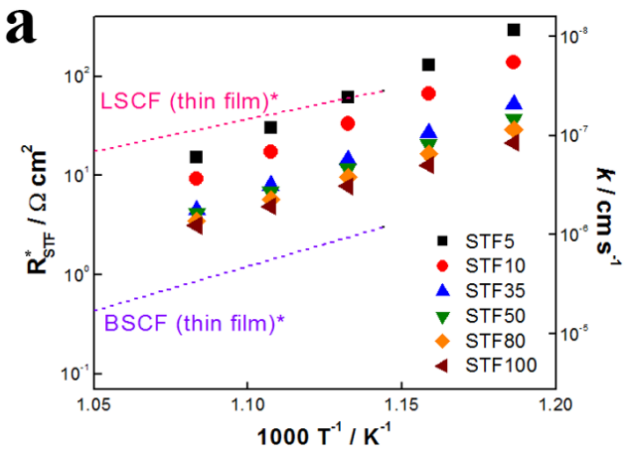

Figure 2. Temperature dependence of R_{STF} for a STF electrode in this work (solid symbols), and other dense thin film MIEC electrodes (LSCF and BSCF) fabricated by PLD (dashed lines). The data for the STF electrodes and for the other MIEC electrodes were obtained respectively from the authors' earlier work [2] and the work of Baumann, et al [11].

Correlation between Oxygen Exchange Kinetics and Transport Properties

While bulk transport kinetics in oxides is well understood, the understanding of interfacial kinetics remains unsatisfactory. Nevertheless, the important role that bulk transport kinetics play in achieving fast oxygen exchange reactions at oxide surfaces have often been reported [12-14]. While it is an accepted rule of thumb that either high electronic or ionic conductivities or both are necessary for obtaining fast oxygen exchange reactions, the fundamental reason for this correlation remains an open question.

To understand the relative role of the bulk transport properties in influencing electrode surface oxygen exchange kinetics, both σ_{el} and σ_{ion} values from bulk STF samples with different Fe compositions are examined and plotted together with respective *k* values in Figure 3. From 5 to 100 mol% Fe, one finds that σ_{el} and σ_{ion} change by nearly five and four orders of magnitudes, respectively, while *k* remains largely within the same order of magnitude. The same trend could be observed when one compares *k* with σ_{el}, obtained from thin film samples. Here one finds also a weak dependence of *k* on σ_{el} with

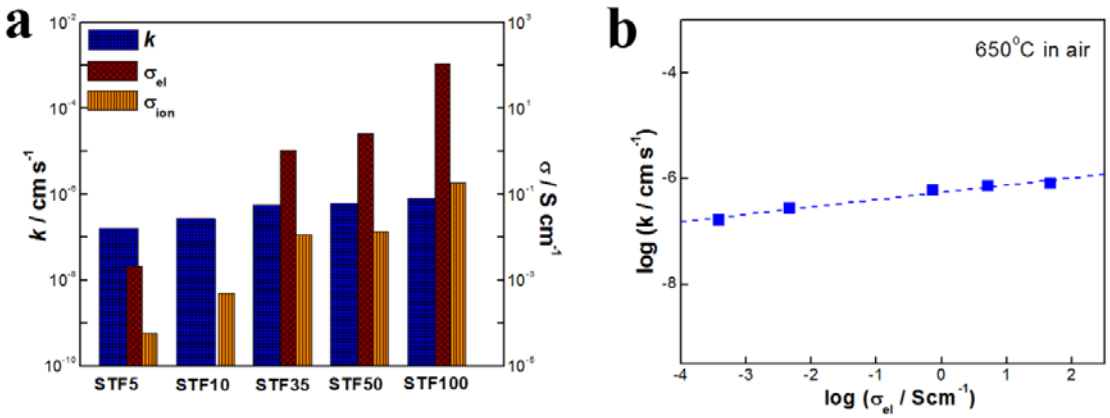

Figure 3. (a) Surface exchange coefficient (*k*), electronic and ionic conductivities (σ_{el} and σ_{ion} for bulk STF) vs. Fe composition at 650°C air. (b) double-logarithmic plot between *k* and σ_{el} (thin film).

with a power law dependence of 0.07 ± 0.02 in a log-log plot. This suggests that oxygen exchange is only weakly correlated with both electronic and ionic transport properties. Furthermore, the activation energy characteristic of *k*, measured by impedance spectroscopy or tracer exchange, was always found to be much greater than those of σ_{el} and σ_{ion}, e.g., E_a (k) of 1.84 eV and E_a (σ_{el}) of 0.17 eV for STF50 thin film. This suggests that the electrical conductivity, at least above a certain minimum value, does not play the limiting role in surface exchange reactions.

Other Factors Governing Oxygen Exchange Kinetics

Surface oxygen exchange requires several electron transfer steps to reduce the oxygen molecule to a doubly charged oxygen ion capable of being inserted into the oxide lattice. Since the combination of both high electronic and ionic transport does not seem to be a critical factor for the exchange kinetics, one may alternatively consider charge transfer as the possible rate determining step (RDS). Determining the efficiency of electron transfer from the catalyst surface to the reactant molecules has been an important topic in the study of catalysts as well as surface science for decades [15-18]. More generally, the electronic band structure, and the corresponding position of the Fermi level (E_F) with respect to the molecular oxygen level or the conduction band edge at the surface, is considered a key factor in governing the rate of electron transfer.

In this work, it was found, surprisingly, that the activation energy of R_{STF} (or *k*) for the surface oxygen exchange reaction and the electronic band gap (E_G^o) of the STF share a similar decreasing trend with increasing Fe composition, as shown in Figure 4. While E_G^o and the activation energy of *k* are not normally considered in the same context, the correlation observed in this study may imply that an electron transfer process must be involved in the RDS for oxygen reduction at the surface of the STF cathode. This is also supported by examining the pO_2 dependent behaviors of the R_{STF} (or *k*). The STF electrodes show a decrease in R_{STF} with increasing pO_2 as commonly observed for perovskite based cathodes. Near ambient air (10^{-2} am < pO_2 < 1 atm), a power law dependence of log R_{STF} on pO_2 in a double-logarithmic plot was observed to be -1/4, known to be typical of the charge transfer reaction (not shown in this manuscript) [14,19,20]. This would be consistent with the transfer rate of minority electronic species being the RDS in this study. This is also consistent with the exchange reaction not being

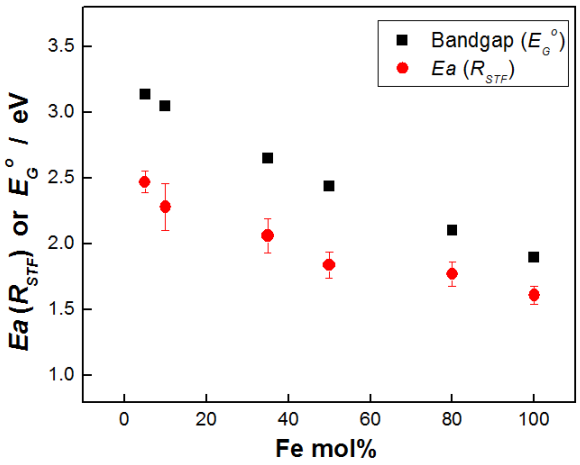

Figure 4. Band gap, E_G^o, (squares) and activation energy of R_{STF} (or *k*) measured by EIS (circle) as a function of Fe composition in air.

strongly dependent on the ionic transport properties or on the majority p-type conductivity. Further confirmation about the correlation between the surface exchange kinetics and the electronic band structure, as well as detailed analysis of the reaction mechanisms on STF electrodes are discussed in a forthcoming publication [21].

Since surface exchange reactions are likely to be highly sensitive to the few atomic layers adjacent to the surface, small change in surface chemistry can be expected to have a significant impact on *k*. Surface segregation by A-site cations in perovskite materials with general chemical formula of ABO_3 has frequently been reported, although the exact role of surface segregation on cathodic performance has not been fully understood [22-25]. Based on XPS chemical analysis, we observed an appreciable degree of SrO-excess, near the surface over the whole composition range studied (see Figure 5a). There are a several important findings regarding SrO segregation to note. First, films with higher Fe fraction tend to have stronger SrO segregation [26]. Second, the degree of SrO segregation can be reduced by chemical etching, but re-segregation, induced by post-annealing etched specimens, is observed at high temperatures (> 600°C) [26]. Lastly, the EIS results under circumstances where a few top atomic layers were removed by chemical etching with dilute HF solution reveal that the SrO segregated layer has a negative impact on *k*, indicating that SrO excess acts as a passivation barrier for the surface oxygen exchange. These findings are consistent with the poor conducting properties of SrO, a wide band gap insulator with E_g of ~ 6 eV [27, 28]. Surface segregation of SrO is therefore considered an important factor in determining the oxygen exchange rate. This feature is under study by STM and XPS [29].

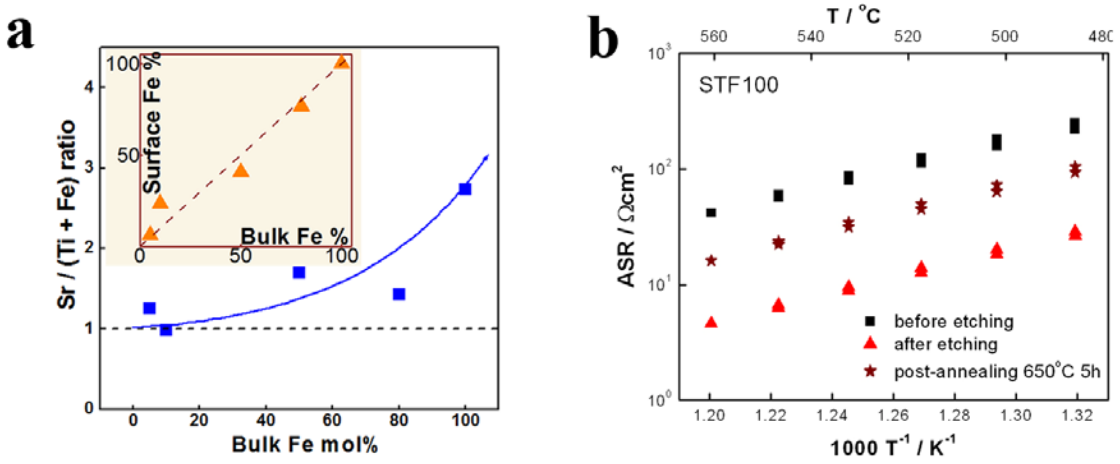

Figure 5. (a) Changes in the ratio between A- and B-site cations after etching the surface of the films or by the Sr deficient film. (b) Effect of post-annealing on the chemically etched STF film (circle) and the Sr deficient film (triangle).

Conclusion

In summary, while metal oxide cathodes for use in solid oxide fuel cells have been the subject of numerous studies, the mechanisms controlling their behavior have remained poorly understood. In this work, a new perovskite materials system was selected, offering the ability to systematically control both the levels of ionic and

electronic conductivity as well as the band structure. This, in combination with considerably simplified electrode geometry, is demonstrated to provide improved insight into the SOFC cathode processes. The observation that the rate of oxygen exchange for mixed conducting cathode materials in SOFC may be largely determined, not by the fast transport properties of the majority electronic and ionic carriers, but by the availability of minority carriers – electrons in the excited state – should aid in directing future research into the physics of these material as well as providing improved guidelines towards the development of cathodes with improved performance at reduced temperatures. This work also points to the importance of understanding and controlling the surface chemistry and physics of the outermost layers of the electrode materials.

Acknowledgments

This work was initially supported by the Ceramics Program, Division of Materials Research Directorate for Mathematical & Physical Sciences, National Science Foundation under award DMR-0243993 and continued under the Materials Science and Engineering Division, Office of Basic Energy Sciences, Department of Energy under award DE SC0002633. W.J. Thanks the Samsung Foundation for fellowship support. The authors thank Dr. R.A. De Souza and Dr. J. Fleig for helpful discussions. The x-ray, XPS and AFM facilities of the Center for Materials Science and Engineering, an NSF MRSEC funded facility, were used in this study.

References

1. W. Jung and H. L. Tuller, *J. Electrochem. Soc.*, **155** B1194 (2008).
2. W. Jung and H. L. Tuller, *Solid State Ion.*, **180** 843 (2009).
3. F. S. Baumann, J. Fleig, H. U. Habermeier, and J. Maier, *Solid State Ion.*, **177** 1071 (2006).
4. A. Rothschild, W. Menesklou, H. L. Tuller, and E. Ivers-Tiffee, *Chem. Mat.*, **18** 3651 (2006).
5. D. J. L. Brett, A. Atkinson, N. P. Brandon, and S. J. Skinner, *Chem. Soc. Rev.*, **37** 1568 (2008).
6. J.-M. Bae and B. C. H. Steele, *Solid State Ion.*, **106** 247 (1998).
7. M. Prestat, J.-F. Koenig, and L. Gauckler, *J. Electroceram.*, **18** 87 (2007).
8. B. C. H. Steele, *J. Power Sources*, **49** 1 (1994).
9. L. W. Tai, M. M. Nasrallah, H. U. Anderson, D. M. Sparlin, and S. R. Sehlin, *Solid State Ion.*, **76** 273 (1995).
10. S. J. Benson, R. J. Chater, and J. A. Kilner, in Proceedings of the 3rd International Symposium on Ionic and Mixed Conducting Ceramics/1997, The Electrochemical Society Proceedings Series, Pennington, NJ.
11. F. S. Baumann, J. Fleig, G. Cristiani, B. Stuhlhofer, H. U. Habermeier, and J. Maier, *J. Electrochem. Soc.*, **154** B931 (2007).
12. B. A. Boukamp, H. J. M. Bouwmeester, and A. J. Burggraaf, in Proceedings of the 2nd International Symposium on Ionic and Mixed Conducting Ceramics/1994, The Electrochemical Society Proceedings Series, Pennington, NJ.
13. R. A. De Souza and J. A. Kilner, *Solid State Ion.*, **126** 153 (1999).
14. R. A. De Souza, *Phys. Chem. Chem. Phys.*, **8** 890 (2006).

15. J. Greeley, J. K. Nørskov, and M. Mavrikakis, *Annu. Rev. Phys. Chem.*, **53** 319 (2002).
16. B. Hammer and J. K. Nørskov, *Nature*, **376** 238 (1995).
17. W.-X. Li, C. Stampfl, and M. Scheffler, *Phys. Rev. Lett.*, **90** 256102 (2003).
18. J. K. Nørskov, J. Rossmeisl, A. Logadottir, L. Lindqvist, J.R. Kitchin, T. Bligaard, and H. Jonsson, *J. Phys. Chem. B*, **108** 17886 (2004).
19. S.B. Adler, *Chem. Rev.*, **104** 4791 (2004).
20. J. Fleig, R. Merkle, and J. Maier, *Phys. Chem. Chem. Phys.*, **9** 2713 (2007).
21. W. Jung and H. L. Tuller, *submitted*.
22. N. Caillol, M. Pijolat, and E. Siebert, *Appl. Surf. Sci.*, **253** 4641 (2007).
23. H. Dulli, P. A. Dowben, S. H. Liou, and E. W. Plummer, *Phys. Rev. B*, **62** R14629 (2000).
24. S. P. Jiang and J. G. Love, *Solid State Ion.*, **138** 183 (2001).
25. S. F. Wagner, C. Warnke, W. Menesklou, C. Argirusis, T. Damjanovic, G. Borchardt, and E. Ivers-Tifee, in Proceedings of the 15th International Conference on Solid State Ionics/2006, Elsevier Science Bv, Baden Baden, Germany.
26. W. Jung and H. L. Tuller, *ECS Trans.*, **25** 2775 (2009).
27. J. Junquera, M. Zimmer, P. Ordej, and P. Ghosez, *Phys. Rev. B*, **67** 155327 (2003).
28. J. A. McLeod, R. G. Wilks, N. A. Skorikov, L. D. Finkelstein, M. Abu-Samak, E. Z. Kurmaev, and A. Moewes, *Phys. Rev. B*, **81** 245123 (2010).
29. Y. Chen, W. Jung, Y. Kuru, H. L. Tuller, and B. Yildiz, submitted to this proceedings (2010).